Numerical Approximation of High-Dimensional Fokker-Planck Equations with Polynomial Coefficients

G. M. Leonenko [a] and T. N. Phillips [b,*]

[a] *School of the Environment and Society, Swansea University, Singleton Park, SA2 8PP, UK*

[b] *School of Mathematics, Cardiff University, Cardiff, CF24 4AG, UK*

Abstract

This paper is concerned with the numerical solution of high-dimensional Fokker-Planck equations related to multi-dimensional diffusion with polynomial coefficients or Pearson diffusions. Classification of multi-dimensional Pearson diffusion follows from the classification of one-dimensional Pearson diffusion. There are six important classes of Pearson diffusion - three of them possess an infinite system of moments (Gaussian, Gamma, Beta) while the other three possess a finite number of moments (inverted Gamma, Student and Fisher-Snedecor). Numerical approximations to the solution of the Fokker-Planck equation are generated using the spectral method. The use of an adaptive reduced basis technique facilitates a significant reduction in the number of degrees of freedom required in the approximation through the determination of an optimal basis using the singular value decomposition (SVD). The basis functions are constructed dynamically so that the numerical approximation is optimal in the current finite-dimensional subspace of the solution space. This is achieved through basis enrichment and projection stages. Numerical results with different boundary conditions are presented to demonstrate the accuracy and efficiency of the numerical scheme.

1 Introduction

The Pearson one-dimensional diffusions defined by linear drift and quadratic squared diffusion coefficient and their ergodic distribution (Gaussian or Gamma

* Corresponding author. Tel.: +44 29 2087 4194; fax: +44 29 2087 4199
Email addresses: G.Leonenko@swan.ac.uk (G. M. Leonenko), PhillipsTN@cf.ac.uk (T. N. Phillips).

or Beta or inverted Gamma or Student or Fisher-Snedecor) satisfies famous Pearson equation (2). The latter three are known as heavy-tailed distributions. It is interesting to note that all of these distributions arise in the theory of classical orthogonal polynomials (with respect to these distributions) in which the systems of orthogonal polynomials are infinite for the first three cases and finite for the heavy-tailed distributions. Their applications can be found in many areas of research such as physical and chemical sciences, engineering, rheology, environmental sciences and financial mathematics.

One possible multidimensional generalization of this class of Pearson diffusions is to consider the high-dimensional FPE with polynomial coefficients. However we restrict our attention to the case when drift is a linear function and squared diffusion has a quadratic form. Applications of such type of models with square diagonal diffusion matrix arise for example in financial mathematics, see Shaw [**?**], Chen Scott [3]. The case becomes much more difficult when square diffusion matrix has full structure since according to the theory instead of classical orthogonal polynomials we have to use their non-commutative analogous, which are matrix-valued. This problem also links to the polynomial solutions of the hypergeometric equations with matrix-valued coefficients where even classification of these orthogonal polynomials is not a trivial task, see Durn and Grnbaum [11],[12]. However bivariate diffusions with non-diagonal matrix have been considered in Shreve [37] wherefore Ornstein-Uhlenbeck (O-U) case the solution is given by using orthogonal transformation which reduces the problem to diagonal case. In Cox-Ingersoll-Ross (CIR) and other problems solutions are not available to the best of our knowledge. Thus, developing numerical methods to these cases seems to be very important task. In this work we only consider the case when square diffusion matrix has a diagonal form for all the Pearson diffusions.

Transient numerical solutions of the one-dimensional FPEs related to Pearson diffusions in the six cases mentioned above for different classifications of the boundary conditions were presented in Leonenko and Phillips [24].

Various discrete time simulation methods have been developed over the years for solutions of one and multi-dimensional stochastic differential equations related to Pearson diffusions. For the most part, investigations have concentrated on solutions for the first three classes, i.e O-U, CIR and Jacobi processes (see Birge and Linetsky [8]). However, analytical investigations and computations for diffusions with so-called heavy-tailed ergodic distributions are more difficult to perform and in the multi-dimensional case have not been attempted. The simulation of solutions of some stochastic differential equations can be problematic due to systematic errors (for example resulting from the discretisation in time) and numerical instabilities. For instance, the diffusion coefficient function could be non-Lipschitz (its derivative becomes infinite as x tends to 0). Another problem with the simulation of SDEs may be the lack

of sufficient numerical stability of the chosen scheme. Also, for theoretically strictly positive processes it is often not acceptable to use discrete time simulation methods that may generate negative values. This problem however, can be solved, in some cases, by a transformation of the initial SDE, via the Ito formula, to a process which lives on the entire real axis. In general, it is a challenging task to obtain efficiently a reasonably accurate trajectory of the square root process using simulation. This has been discussed in the literature below using the balanced implicit method introduced by Milstein et al. [28], the adaptive Milstein scheme [20] and the balanced Milstein method [1], for example. Discretisation schemes dedicated to square root diffusions have also been studied in recent years by Alfonsi [2], Kahl and Schurz [21] and Andersen [6].

In this paper we consider multi-dimensional FPEs related to Pearson diffusions which potentially have number of advantages. First of all the solution of a FPE gives us the exact density, instead of just simulating the path of a stochastic process. Second, we do not need to deal with the problem of negativity of the square root in the diffusion term, see discussion in Leonenko and Phillips [24]. Third, application of spectral numerical techniques provide us with accurate solutions which can be calculated very efficiently using a relatively small number of discretisation points.

Needless to say the FPE (forward Kolmogorov equation) is one of the most fundamental equations in physics and plays an important role in every area of science. However, despite of this importance there remains many unresolved analytical and numerical problems. Analytical solutions of the FPEs are available for only a few special cases. Numerical solutions are possibilities but pose formidable challenges. Various numerical methods like the path integral method [29,22], Galerkin method, finite element method, finite difference method and multi-scale finite element method have been developed to solve the Fokker-Planck equation.

In this paper an adaptive reduced basis approximation to the FPE is constructed using an efficient separation of variables technique. The method was introduced by Ammar et al. [4,5] in the context of the finite element method and further were developed by Leonenko and Phillips [23] in the context of high-order spectral approximations. This approach based on singular value decomposition (SVD) and gives us efficient basis reduction since it provides a mechanism for retaining only those basis functions that contain the most representative information of the solution in the numerical approximation. Therefore, the method allows us to reduce the number of degrees of freedom. The novelty of this work is in the use of spectral approximations combined with a dynamic construction of the basis to achieve optimal approximations in a least squares sense of the multi-dimensional FPEs related to Pearson diffusions.

The paper is organized in the following way: after introduction in the second section high-dimension FPE and eigenvalue problem is presented with the classification . In the third section the adaptive reduced basis approximation for two-dimension case is introduced which involves two stages (projection and enrichment). In the forth section this approach is extended for d-dimension case of the FPE. Fifth section is devoted to the numerical and comparison results for each of the six cases followed by discussion section.

2 High-dimension Fokker-Planck representation

In this paper we investigate Pearson-like diffusions in high-dimensions using the reduced basis method. Thus, we consider the following FPE:

$$\frac{\partial p(\mathbf{x},t)}{\partial t} = -\sum_{i=1}^{d} \frac{\partial}{\partial x_i} a(\mathbf{x}) p(\mathbf{x},t) + \frac{1}{2} \sum_{i=1}^{d} \sum_{j=1}^{d} \frac{\partial^2}{\partial x_i \partial x_j} \left(\sigma_{ij}(\mathbf{x})\right) p(\mathbf{x},t) \qquad (1)$$

where $p(\mathbf{x},t) = p(\mathbf{x};\ \mathbf{x_0},t)$ is the transition density of the corresponding d-dimensional Markov process with the linear drift: $a(\mathbf{x}) = (a(x_1),...,a(x_d))$ and the quadratic square diffusion term: $D = (\sigma_{ij}(\mathbf{x}))_{1\le i,j\le d} =< \Sigma\mathbf{x},\mathbf{x} >$ is a symmetric and non-negatively defined $d \times d$ matrix where $\sigma(\mathbf{x}) = 2d(\mathbf{x})$,

Pearson [33] classifies invariant densities $m(\cdot)$ of the one-dimensional eq. (1) using the following differential equation

$$\frac{m'(x)}{m(x)} = \frac{a(x) - d'(x)}{d(x)} = \frac{(a_1 - 2b_2)x + (a_0 - b_1)}{b_2x^2 + b_1x + b_0} = \frac{q(x)}{d(x)} \quad x \in \mathbb{R}, \qquad (2)$$

where $q(x)$ and $d(x)$ are linear and quadratic functions, respectively. It seems appropriate to call this important class of processes, Pearson diffusions.

A classification of Pearson diffusions (Forman, Sørensen[14]) in terms of six basic sub-families may be achieved using criteria based on the degree, $\deg(d)$, of the polynomial $d(x)$ appearing in the denominator of the Pearson equation (2) and the sign of the leading coefficient b_2. The discriminant $\Delta(d)$ in the quadratic case is $\Delta(d) = b_1^2 - 4b_2b_0$.

The classification for the multi-dimensional case can be written as:

$$\frac{q_i(x_i)}{d_i(x_i)} = \frac{a_{1,i}x_i + a_{0,i}}{b_{2,i}x_i^2 + b_{1,i}x_i + b_{0,i}}, \quad x_i \in \mathbb{R},\ i = 1,...,d. \qquad (3)$$

The classification below is for the one-dimensional case, but in our work we extend it to the corresponding d-dimensional FPE. Introducing classes of multi-dimensional diffusions where each linear function q_i in the numerator and

quadratic function d_i in denominator belongs to the classification scheme of one-dimensional Pearson diffusion for $i = 1, \ldots, d$ (see Forman and Sørensen [14]).

The six cases can be described in the following way:

(1) Ornstein-Uhlenbeck: $\deg(d) = 0$; invariant density is normal.
(2) CIR diffusion: $\deg(d) = 1$; invariant density is gamma.
(3) Jacobi diffusion: $b_2 < 0; \deg(d) = 2; \Delta(d) > 0$; invariant density is beta.
(4) Fisher-Snedecor diffusion: $b_2 > 0; \deg(d) = 2; \Delta(d) > 0$; invariant density is Fisher-Snedecor.
(5) Reciprocal gamma diffusion: $b_2 > 0; \deg(d) = 2; \Delta(d) = 0$; invariant density is reciprocal gamma.
(6) Student diffusion: $b_2 > 0; \deg(d) = 2; \Delta(d) < 0$; invariant density is Student.

In general, the solution of eq. (1) is a challenging problem. However, for a diagonal matrix D (this means that the Brownian motions of the multidimensional diffusions are independent) one can proceed further. For simplicity we consider the situation where the eigenvalue problem has a pure discrete spectrum.

Recall that the Itô stochastic differential equivalent equation is of the form

$$d\mathbf{X}_t = a(\mathbf{X}_t)dt + \sqrt{\sigma(\mathbf{X}_t)}d\mathbf{B}_t,\ t \geq 0, \tag{4}$$

where $\mathbf{B} = (B_t^{(i)},\ i = 1, ..., d)$ is a d-dimensional Brownian motion and

$$\mu(\mathbf{x}) = (\mu(x_i),\ i = 1, \ldots, d)$$

is a $d \times 1$ Borel measurable vector and $\sqrt{\sigma} = (\sqrt{\sigma_{ij}(\mathbf{x})})_{1 \leq i,j, \leq d}$ is a $d \times d$ Borel measurable positive definite matrix.

We assume that the coefficients of the diffusion satisfy the Lipschitz and growth conditions:

(i) there exist constants C_1 and C_2 such that for all x and y

$$\|a(\mathbf{x}) - a(\mathbf{y})\| + \left\|\sqrt{\sigma(\mathbf{x})} - \sqrt{\sigma(\bar{y})}\right\| \leq C_1 \|\mathbf{x} - \mathbf{y}\|, \tag{5}$$

and

$$\|a(\mathbf{x})\| + \left\|\sqrt{\sigma(\mathbf{x})}\right\| \leq C_2\{1 + \|\mathbf{x}\|\}, \tag{6}$$

where $\|\sqrt{\sigma}(\mathbf{x})\| = \sqrt{\sum_{i=1}^d \sum_{j=1}^d \sigma_{ij}^2(\mathbf{x})}$ and $\|a(\mathbf{x})\| = \sqrt{\sum_{i=1}^d a_i^2(\mathbf{x})}$.

Under these considerations, the SDE (4) has a unique strong solution. Note that these conditions hold in most of the cases. Otherwise (for instance Jacobi

diffusion) we have to use some other conditions, (see Gihman and Skorohod [17]), or interpret solutions in a weak sense and ergodicity follows from the Feller conditions under the assumption of the parameters chosen below, (see Bibby et al.[7]).

Let us consider the infinitesimal generator

$$\mathcal{G}f = \frac{1}{2}\sum_{i,j=1}^{d} \sigma_{ij}(x_{ij})\frac{\partial^2 f}{\partial x_i \partial x_j} + \sum_{i=1}^{d} a(x_i)\frac{\partial f}{\partial x_i},$$

on the set $E = \{f \in L^1(\mathbb{R}^d) \cap C_b^2(\mathbb{R}^d) :\ Gf \in L^1(\mathbb{R}^d)\}$, where $C_b^2(\mathbb{R}^d)$ denotes the set of all twice differentiable bounded functions whose derivatives of order ≤ 2 are continuous and bounded.

Note that the infinitesimal generator of $\mathbf{X_t}$ is defined to act on suitable functions $f :\ \mathbb{R}^d \to \mathbb{R}$

$$Gf(\mathbf{x}) = \lim_{t \downarrow 0} \frac{E^{\mathbf{x}}[f(\mathbf{X}_t)] - f(\mathbf{x})}{t}. \tag{7}$$

If $v \in C_b^2(\mathbb{R}^d)$ then equation (1) has in any time interval $[0, T]$ a unique classical solution which satisfies the initial condition $p(\mathbf{x}, 0) = v(\mathbf{x})$, and this solution and its spatial derivatives up to order 2 are uniformly bounded on $[0, T] \times \mathbb{R}^d$ [17,32] .

From the Gauss-Ostrogradski theorem it follows that the integral $\int p(\mathbf{x}, t)d\mathbf{x}$ is constant. Let $P(t)$ be a Markov semigroup, that is $P(t)v(\mathbf{x}) = p(\mathbf{x}, t)$ for $v \in C_c^2(\mathbb{R}^d)$ and $t \geq 0$, since the operator $P(t)$ is a construction on $L^1(\mathbb{R}^d)$. We have $P(t)\left(C_c^2(\mathbb{R}^d)\right) \subset C_b^2(\mathbb{R}^d),\ t \geq 0$.

According to Proposition 1.3.3. in Griffiths, Spano [18] the closure of the operator G generates the semigroup $\{P(t)\}_{t\geq 0}$. The adjoint operator $\{P^*(t)\}_{t\geq 0}$ forms a semigroup on $L^\infty(\mathbb{R}^d)$ given by the formula

$$P^*(t)g(\mathbf{x}) = \int_{R^d} g(\mathbf{y})P(t, \mathbf{x}, d\bar{y}),\ g \in L^\infty(\mathbb{R}^d), \tag{8}$$

where $P(t, \mathbf{x}, A)$ is the transition probability function of the diffusion process $\mathbf{X}_t$, i.e.

$$P(t, \mathbf{x}, A) = P\{\mathbf{X}_t \in A\} = \int_A p(\mathbf{x}, t)d\mathbf{x}. \tag{9}$$

In the case where Brownian motions $B_t^{(i)}$, $i = 1, \ldots, d$, are independent or the matrix D is diagonal, we take $\mathbf{X}_t = (X_t^{(i)}, i = 1, \ldots, d)$, where $X_t^{(i)}$ is a one-dimensional independent diffusion. The infinitesimal generator and its eigenvalue spectral problem reduces to the eigenvalue problems of generators G_i of each one-dimensional diffusion $X_t^{(i)}, t \geq 0$, $i = 1, \ldots, d$.

The corresponding eigenvalue problem for a generator of multidimensional diffusions $G = (G_1, \ldots, G_d)$ has a hypergeometric form

$$G_i f_{n_i}^{(i)} + \lambda_{n_i}^{(i)} f_{n_i}^{(i)} = 0, \; i = 1, ..., d, \tag{10}$$

for a multi-index $n = (n_1, \ldots, n_d) \in \mathbb{Z}_+^d$. The eigenfunctions have a product form: $f_n = f_{n_1} \times ... \times f_{n_d}$ and eigenvalues $\lambda_n^{(i)} = \lambda_{n_1}^{(i)} + \ldots + \lambda_{n_d}^{(i)}$, where for $i = 1, \ldots, d$, $\lambda_0^{(i)} < \lambda_1^{(i)} < \cdots \lambda_l^{(i)}$, $\lim\limits_{l \to \infty} \lambda_l^{(i)} = \infty$.

Note that in this case the ergodic measure is formed of product of components: $\mu = \mu_1 \times \cdots \times \mu_d$, and we denote $m(\mathbf{x})$ its Radon-Nikodym derivatives.

Then, the spectral representation of the transition density of the multidimensional diffusion with the linear drift and quadratic square diffusion takes the following form in the case of a pure discrete spectrum:

$$p(\mathbf{x};\, \mathbf{x}_0, t) = m(\mathbf{x}) \sum_{n \in \mathbb{Z}_+^d} e^{-\lambda_n t} f_n(\mathbf{x}) f_n(\mathbf{x}_0), \tag{11}$$

where $p(\mathbf{x}; \mathbf{x}_0, t) = \frac{\partial}{\partial \mathbf{x}} P(\mathbf{X}_t \leq \mathbf{x} | \mathbf{X}_0 = \mathbf{x}_0)$. Thus, for example, in the Hermite case $f_n(\mathbf{x}) = H_{n_1}(x_1) \times \cdots \times H_{n_d}(x_d)$ is a product of corresponding one-dimensional orthogonal polynomials. Similar expressions can be written down for Laguerre and Jacobi polynomials. The situation for heavy-tailed multidimensional diffusions is very complicated due to the difficulties related to the continuous part of the spectrum.

Note, that in this case the classification of the boundary points is similar to the one-dimensional case (see Meerschaert [27], Leonenko Phillips [24]). Classical results for the Feller classification can be found in Ito and McKean [19] and for the oscillatory/non-oscillatory and Weyl's limit-point/limit-circle classifications in Fulton et al. [15].

3 Numerical approximation of the Fokker-Planck equation

In this section we present a spectral approximation to the solution of the d-dimensional FPE (1) by expressing $p(\mathbf{x}, t)$ in terms of a reduced basis approximation. Thus, we consider the FPE (1) for the conditional density, $p(\mathbf{x}, t)$, of the variable $\mathbf{X}_t = \mathbf{x} | \mathbf{X}_{t_0} = \mathbf{x}_0$ of the corresponding homogeneous Markov process with the state space, Ω, that is, for any initial $\mathbf{x}_0$, t_0, with the initial condition

$$p(\mathbf{x}, t)|_{t=t_0} = \delta(\mathbf{x} - \mathbf{x}_0). \tag{12}$$

However, using the definition of the conditional probability one can see that it is also valid for $p(\mathbf{x}, t)$ with the initial condition

$$p(\mathbf{x}, t)|_{t=t_0} = p(\mathbf{x}, t_0) \tag{13}$$

which is less singular than (12). In other words, the numerical solution is not sensitive to the choice of initial condition and therefore we can choose the initial condition to be any integrable function in Ω.

The domain $\Omega \subset \mathbb{R}^d$ is transformed into the computational domain $[-1, 1]^d$ using the mapping

$$x_{i,new} = \frac{2x_i}{L} - 1, \; x_{i,new} \in [-1, 1], \; i = 1, \ldots, d.$$

To simplify notation we drop the 'new' subscripts for x.

The weak formulation of the equation (1), after the time derivative has been approximated using the backward Euler scheme, is

$$\int_\Omega p^* \left(\frac{p(\mathbf{x}, t^{n+1}) - p^n(\mathbf{x}, t^n)}{\Delta t} \right) \, d\Omega + \sum_{i=1}^{d} \int_\Omega p^* \frac{\partial}{\partial x_i} [a_i(\mathbf{x}) p(\mathbf{x}, t^{n+1})] \, d\Omega$$
$$- \frac{1}{2} \sum_{i=1}^{d} \sum_{j=1}^{d} \int_\Omega p^* \frac{\partial^2}{\partial x_i \partial x_j} \left[\sigma_{ij}(\mathbf{x}) p(\mathbf{x}, t^{n+1}) \right] \, d\Omega = 0 \tag{14}$$

for all test functions p^* in some appropriate function space. In equation (14), Δt is the time step and $t^n = n\Delta t$.

The approximation to the solution of this problem is sought in the form

$$p(\mathbf{x}, t^{n+1}) = \sum_{j=1}^{J} \alpha_j^{n+1} g_j^{1,(n+1)}(x_1) \times \ldots \times g_j^{d,(n+1)}(x_d), \tag{15}$$

where the basis functions corresponding to each of the d independent variables $\mathbf{x} = (x_1, \ldots, x_d)$, have the form

$$g_j^{l,(n+1)}(x_l) = \sum_{k=1}^{N-1} g_{j,k}^l h_k(x_l), \quad l = 1, \ldots, d,$$

and $g_{j,k}^l = g_j^l(\xi_k)$ are coefficients which are determined in the enrichment stage. In the case of an approximation of degree N, the interpolating polynomials h_k are defined by

$$h_k(\xi) = -\frac{(1 - \xi^2) L_N'(x)}{N(N+1) L_N(\xi_k)(\xi - \xi_k)} \tag{16}$$

where $L_N(x)$ is the Legendre polynomial of degree N and ξ_k, $0 \leq k \leq N$ are the Gauss-Lobatto Legendre (GLL) nodes. The polynomials $h_k(\xi)$ satisfy the Kronecker delta property $h_k(\xi_j) = \delta_{kj}$. The entries of the Legendre collocation differentiation matrix, $\hat{D}_N$, are given explicitly by

$$(\hat{D}_N)_{j,k} = h'_k(\xi_j) = \begin{cases} \frac{L_N(\xi_j)}{L_N(\xi_k)} \frac{1}{\xi_j - \xi_k} & j \neq k \\ -\frac{(N+1)N}{4} & j = k = 0 \\ \frac{(N+1)N}{4} & j = k = N \\ 0 & \text{otherwise.} \end{cases} \tag{17}$$

The corresponding test function is:

$$p^*(\mathbf{x}, t^{n+1}) = \sum_{j=1}^{J} \alpha_j^{n*,(n+1)} g_j^{1,(n+1)}(x_1) \times \cdots \times g_j^{d,(n+1)}(x_d). \tag{18}$$

For simplicity we drop the superscript $n+1$ on α_j and $g_j(x)$ for $j = 1, \ldots, J$.

As a result of the separation of variables (15), the integral of p over configuration space Ω_x can be expressed as the product of d one-dimensional integrals

$$\int_{\Omega_x} p(\mathbf{x})\, d\mathbf{x} = \sum_{j=0}^{\infty} \alpha_j \left(\prod_{l=1}^{d} \int_{-1}^{1} g_j^l(x_l) dx_l \right).$$

To evaluate each of the one-dimensional integrals we use the Gauss quadrature rule

$$\int_{-1}^{1} f(\xi) d\xi \simeq \sum_{j=0}^{N} f(\xi_j) w_j^N, \tag{19}$$

where ξ_j, $0 \leq j \leq N$, are the GLL nodes and the weights, w_j^N, are defined by

$$w_j^N = \frac{2}{N(N+1)(L_N(x_j))^2}. \tag{20}$$

The procedure for determining the numerical approximation comprises two stages. We iteratively construct basis functions $g_j^l(x_l)$, $l = 1, \ldots, d$ with an optimal rank J [23]. In the projection stage, the values of α_j, $j = 1, \ldots, J$, are computed. This is followed by an enrichment of the basis by calculating additional basis functions $g_{J+1}^l(x_l)$, $l = 1, \ldots, d$, in the enrichment stage. This method proceeds in an iterative manner until convergence is obtained. Convergence is obtained once the absolute value of α_J falls below some prescribed tolerance [23].

3.1 Projection Stage

The purpose of the projection stage is to compute the coefficients α_j, $j = 1, \ldots, J$, in the reduced basis representation for p_N in (15). In this stage, the basis functions $g_j^l(x_l)$, $j = 1, \ldots, J$, $l = 1, \ldots, d$, are known. Thus, inserting the approximation (15) into the weak formulation of the problem (14) and simplifying the result yields the linear system

$$M\alpha = \mathbf{v}, \tag{21}$$

where M is the diagonal matrix with entries

$$M_{i,i} = 1 + \Delta t \left\{ \sum_{k=1}^{d} (\mathbf{g}_i^k)^T A \mathbf{g}_i^k \right\} \tag{22}$$

and the entries of the vector $\mathbf{v}$ are given by

$$v_i = \sum_{j=1}^{J} \alpha_j^n \prod_{k=1}^{d} (\mathbf{g}_i^k)^T B \mathbf{g}_i^{k,n} \tag{23}$$

The $N \times N$ matrices A and B are defined by

$$A_{m,n} = -w_n a_n(\mathbf{x})(\hat{D}_N)_{n,m} + \frac{1}{2} \sum_{l=1}^{N} \boldsymbol{\sigma}_{ll}(\mathbf{x}) w_l (\hat{D}_N)_{l,m} (\hat{D}_N)_{l,n}, \tag{24}$$

$$B_{m,n} = w_m \delta_{m,n}, \tag{25}$$

respectively.

The basis functions $\{\mathbf{g}_k^d\}$ are constructed to be B-orthonormal i.e.

$$\mathbf{g}_i^d B \mathbf{g}_j^d = \delta_{i,j}$$

where δ is the Kronecker delta. Therefore, the matrix M is a diagonal matrix.

3.2 Enrichment Stage

In this stage, the basis functions $g_j^1(x_1), \ldots, g_j^d(x_d)$ and coefficients α_j, $j = 1, \ldots, J$, are known. The basis is enriched by adding an additional basis function $r^1(x_1) \ldots r^d(x_d)$. The approximation is then written in the form

$$p(\mathbf{x}, t^{n+1}) = \sum_{j=1}^{J} \alpha_j g_j^1(x_1) \ldots g_j^d(x_d) + r^1(x_1) \ldots r^d(x_d). \tag{26}$$

The corresponding test function in this stage has the following representation

$$p^*(\mathbf{x}, t^n) = r^{1*}(x_1)\dots r^d(x_d) + \dots + r^1(x_1)\dots r^{d*}(x_d). \tag{27}$$

The structure of $r^1(x_1), \dots, r^d(x_d)$ is the same as for $g^1(x_1), \dots, g^d(x_d)$, respectively. Inserting (26) and (27) into (14) yields the nonlinear problem

$$\mathbf{v}_1(\mathbf{r}^1, \mathbf{r}^2, \dots, \mathbf{r}^d) + Z(\mathbf{r}^1, \mathbf{r}^2, \dots, \mathbf{r}^d) \begin{bmatrix} \mathbf{r}^1 \\ \mathbf{r}^2 \\ \vdots \\ \mathbf{r}^d \end{bmatrix} = \mathbf{v}_2(\mathbf{r}^1, \mathbf{r}^2, \dots, \mathbf{r}^d). \tag{28}$$

This system is of dimension $N \times d$ and must be solved using a suitable iterative scheme. The simplest scheme which also turns out to be robust is the so-called alternating direction, fixed-point algorithm. Each iteration consists of d steps that are repeated until convergence is reached and the fixed point has been found.

We present this algorithm in the case when $d = 2$. In this case the $2N \times 2N$ matrix Z can be partitioned as follows

$$Z(\mathbf{r}^1, \mathbf{r}^2) = \begin{bmatrix} A(\mathbf{r}^2)^T B\mathbf{r}^2 & B\mathbf{r}^1(\mathbf{r}^2)^T A \\ B\mathbf{r}^2(\mathbf{r}^1)^T A & A(\mathbf{r}^1)^T B\mathbf{r}^1 \end{bmatrix}.$$

and the vectors $\mathbf{v}_1$ and $\mathbf{v}_2$ are defined by

$$\mathbf{v}_1(\mathbf{r}^1, \mathbf{r}^2) = \sum_{j=1}^{J} \alpha_j \begin{bmatrix} A\mathbf{g}_j^1(\mathbf{r}^2)^T B\mathbf{g}_j^2 + B\mathbf{g}_j^1(\mathbf{r}^2)^T A\mathbf{g}_j^2 \\ (\mathbf{r}^1)^T A\mathbf{g}_j^1 B\mathbf{g}_j^2 + (\mathbf{r}^1)^T B\mathbf{g}_j^1 A\mathbf{g}_j \end{bmatrix},$$

$$\mathbf{v}_2(\mathbf{r}^1, \mathbf{r}^2) = \sum_{j=1}^{J} \alpha_j^{(n)} \begin{bmatrix} g_j^{1,n}(x_1) w (g_j^{2,n}(x_2))^T w g_j^{2,n}(x_2) \\ g_j^{2,n}(x_2) w (g_j^{1,n}(x_1))^T w g_j^{1,n}(x_1) \end{bmatrix}.$$

To solve the system (28) we use the efficient non-linear solver which we describe below, i.e.

Instead of solving a nonlinear system of dimension $2N$, we solve the associated pair of linear systems of dimension N using an alternating direction iteration procedure. To describe this, let us rewrite the system (28) as

$$\begin{pmatrix} \mathbf{v}_1(\mathbf{r}^2) \\ \mathbf{v}_1(\mathbf{r}^1) \end{pmatrix} + \begin{pmatrix} Z_{11}(\mathbf{r}^2) & Z_{12}(\mathbf{r}^1, \mathbf{r}^2) \\ Z_{21}(\mathbf{r}^1, \mathbf{r}^2) & Z_{22}(\mathbf{r}^1) \end{pmatrix} \begin{pmatrix} \mathbf{r}^1 \\ \mathbf{r}^2 \end{pmatrix} = \begin{pmatrix} \mathbf{v}_2(\mathbf{r}^2) \\ \mathbf{v}_2(\mathbf{r}^1) \end{pmatrix}. \tag{29}$$

Then the iterative scheme comprises the following two steps:

(1) Suppose that we have an approximation to $\mathbf{r}^2$, solve the linear system

$$Z_{11}(\mathbf{r}^2)\mathbf{r}^1 = \mathbf{v}_2(\mathbf{r}^2) - \mathbf{v}_1(\mathbf{r}^2) - Z_{12}(\mathbf{r}^1, \mathbf{r}^2)\mathbf{r}^2, \tag{30}$$

and normalise the solution

$$\overline{r}^1_{new} = \frac{\mathbf{r}^1}{\sqrt{(\mathbf{r}^1)^T B \mathbf{r}^1}}$$

(2) With the new approximation to $\mathbf{r}^1$, solve the linear system

$$Z_{22}(\mathbf{r}^1)\mathbf{r}^2 = \mathbf{v}_2(\mathbf{r}^1) - \mathbf{v}_1(\mathbf{r}^1) - Z_{21}(\mathbf{r}^1, \mathbf{r}^2)\mathbf{r}^1, \tag{31}$$

then normalise $\overline{r}^2$

$$\overline{r}_{2new} = \frac{\mathbf{r}^2}{\sqrt{(\mathbf{r}^2)^T B \mathbf{r}^2}}.$$

After the iterative process (30)-(31) has converged, the new basis functions $g^1_{J+1}(x_1)$ and $g^2_{J+1}(x_2)$ are constructed from $r^1(x_1)$ and $r^2(x_2)$, respectively, to obtain orthonormal bases through the Gram-Schmidt orthogonalization process:

$$g^1_{J+1}(x_1) = r^1(x_1) - \sum_{j=1}^{J}((\mathbf{r}^1)^T B \mathbf{g}^1_j) g^1(x_1),$$
$$g^2_{J+1}(x_2) = r^2(x_2) - \sum_{j=1}^{J}(\mathbf{r}^2)^T B \mathbf{g}^2_j) g^2_j(x_2).$$

The extension for general d follows in a straightforward fashion and the procedure involves the solution of d linear systems each of dimension N and therefore is a much cheaper alternative to the solution of the full nonlinear system. The solution of this system yields the values of $r^1(x_1), \ldots, r^d(x_d)$, at the GLL points and hence the new basis function is determined. Furthermore, the normality of the configuration pdf requires that one of the integrals should vanish i.e.

$$\int_0^L r^k(x_k)\, dx_k = 0, \quad \text{for one of } \; k = 1, \ldots, d.$$

The solution is normalized so that

$$\mathbf{r}^k_{new} = \frac{\mathbf{r}^k}{\sqrt{(\mathbf{r}^k)^T B \mathbf{r}^k}}, \quad k = 1, \ldots, d.$$

4 Pearson diffusions

4.1 Ornstein-Uhlenbeck process

This diffusion is transient OU process (also known in the financial literature as the Vasiček model in one dimension). In the high-dimensional case the FPE has the form:

$$\frac{\partial p(\mathbf{x},t)}{\partial t} = -\sum_{i=1}^{d} \frac{\partial}{\partial x_i}(a_i - b_i x_i)p(\mathbf{x},t) + \frac{1}{2}\sum_{i=1}^{d}\sum_{i=1}^{d} \frac{\partial^2}{\partial x_i^2}\sigma_{ii}^2 p(\mathbf{x},t), \tag{32}$$

defined on $(-\infty,\infty)^n$ and $a_i \in \mathbb{R}$, $b_i > 0$, $\sigma_{ii} \in \mathbb{R}^+$, where $i = 1,\ldots,d$ with eigenvalues $\lambda_n = \lambda_{n1}^{(1)} + \cdots + \lambda_{nd}^{(d)} = n_1 b_1 + \cdots + n_d b_d$.

The ergodic distribution for each of the components is Gaussian:

$$X_t^{(i)} \sim N\left(\frac{a_i}{b_i}, \frac{\sigma_{ii}}{2b_i}\right).$$

The boundary conditions $D_i^1 = -\infty$ and $D_i^2 = +\infty$, $i = 1,\ldots,d$ are natural boundaries for all choices of parameters.

The corresponding eigenfunctions in this case are Hermite polynomials (see [9], for example). And the transition probability density has the expansion

$$p(\mathbf{x}_1;\, \mathbf{x}_0, t) = \prod_{i=1}^{d} \frac{1}{\sqrt{\frac{\pi\sigma_{ii}^2}{b_i}}} \exp\left(-\frac{b_i}{\sigma_{ii}^2}\left(x_i - \frac{a_i}{b_i}\right)^2\right) \times$$

$$\sum_{n_1=0}^{\infty}\cdots\sum_{n_d=0}^{\infty} \frac{e^{-(n_1 b_1 + \cdots + n_d b_d)t}}{2^{n_1+\cdots+n_d} n_1! \times \cdots \times n_d!} \prod_{i=1}^{d} H_n\left(y_{i,0}\right) \prod_{i=1}^{d} H_n\left(y_{i,1}\right),$$

where

$$y_{i,j} = \sqrt{\frac{b_i}{\sigma_{ii}^2}}\left(x_{i,j} - \frac{a_i}{b_i}\right),\ i = 1,\ldots,d,\ j = 0,1.$$

Also we can write the transient solution in terms of the Gaussian distribution as follows:

$$p(\mathbf{x};\mathbf{x}_0,t) = \prod_{i=1}^{d} \frac{1}{\sqrt{\frac{\pi\sigma_{ii}^2}{b_i}(1-e^{-2b_i t})}} \exp\left(-\frac{\left(x_i - \frac{a_i}{b_i} - (x_{i,0} - \frac{a_i}{b_i})e^{-b_i t}\right)^2}{\frac{\sigma_{ii}^2}{b_i}(1-e^{-2b_i t})}\right). \tag{33}$$

In high-dimensional cases it is useful to compare the results through the ex-

pectation of the time-dependent solution:

$$E(t) = \int_{\mathbb{R}^d} \left(\sum_{i=1}^{d} \right) x_i p(\mathbf{x}, t)\, \mathbf{dx} = \sum_{i=1}^{d} \left(\frac{a_i}{b_i} + (x_{i,0} - \frac{a_i}{b_i}) e^{-b_i t} \right). \qquad (34)$$

In Fig. 1 (a) we plot the numerical solution of the 2-D FPE (32) when it converges to the steady-state solution, obtained using a spectral approximation with $N = 80$. The model parameters were chosen to be $a_1 = 3$, $a_2 = 6$, $b_1 = 2$, $b_2 = 3$ and $\sigma_{11}^2 = 1$, $\sigma_{22}^2 = 0.5$, $x_0 = 2.6$. The boundary conditions are natural. Two basis functions are sufficient to represent the solution, $\alpha_0 = 11.9902$, $\alpha_1 = 4.956 \times 10^{-5}$. The exact solution to the problem is shown in Fig. 1 (b). Excellent agreement is obtained confirming that the spectral approximation is able to provide an accurate representation of solutions to this equation. Fig. 1 (c) presents a comparison between numerical and analytical first moment (see (34)).

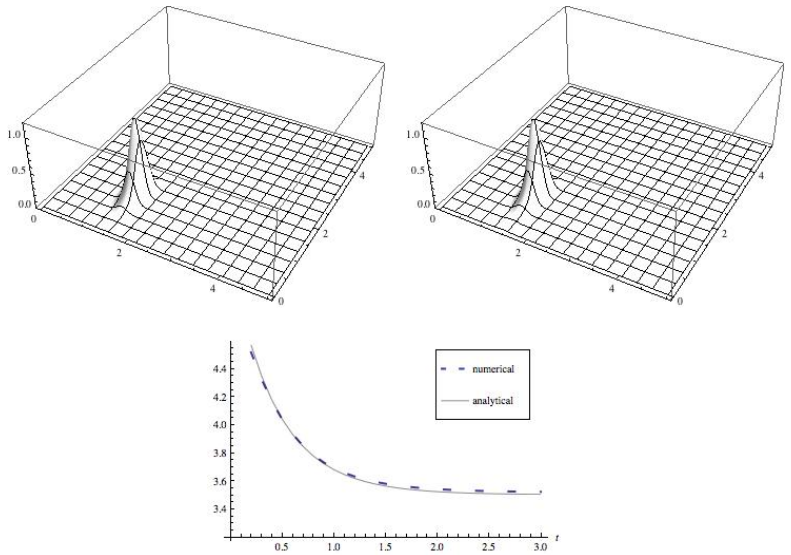

Figure 1. Ornstein-Uhlenbeck process with $a_1 = 3$, $a_2 = 6$, $b_1 = 2$, $b_2 = 3$ and $\sigma_{11}^2 = 1$, $\sigma_{22}^2 = 0.5$, $x_0 = 2.6$. Boundary conditions are natural. (a) Numerical approximation obtained using reduced basis approach. (b) Analytical solution. (c) Comparison between numerical and analytical expectations.

In Fig. 2 we plot the comparison of the expectation for the 3-D FPE (32) with natural boundary conditions for the spectral approximation with $N = 80$ and the analytical solution (34) with $x_0 = 2.5$. The model parameters were chosen to be $a_1 = 3$, $a_2 = 6$, $a_3 = 7$, $b_1 = 2$, $b_2 = 3$, $b_2 = 4$ and $\sigma_{11}^2 = 1$, $\sigma_{22}^2 = 0.5$, $\sigma_{22}^2 = 0.7$, $x_0 = 2.7$. To obtain a solution at steady state only two basis function are sufficient to represent the solution with $\alpha_0 = 34.9308$, $\alpha_1 = 1.7333 \times 10^{-9}$.

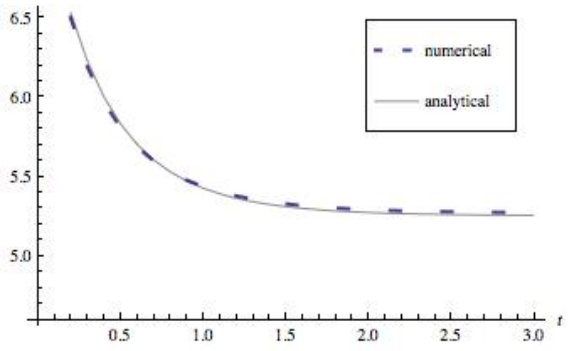

Figure 2. Comparison between the numerical and analytical expectations for the Ornstein-Uhlenbeck process in 3-D with $a_1 = 3$, $a_2 = 6$, $a_3 = 7$, $b_1 = 2$, $b_2 = 3$, $b_2 = 4$ and $\sigma_{11}^2 = 1$, $\sigma_{22}^2 = 0.5$, $\sigma_{22}^2 = 0.7$, $x_0 = 2.7$.

4.2 The square root/CIR process

In financial mathematics this process is known as the CIR process (see Birge and Linetsky [8]). The FPE is

$$\frac{\partial p(\mathbf{x},t)}{\partial t} = -\sum_{i=1}^{d} \frac{\partial}{\partial x_i}(a_i - b_i x_i)p(\mathbf{x},t) + \frac{1}{2}\sum_{i=1}^{d} \frac{\partial^2}{\partial x_i^2}\sigma_{ii}^2 x_i p(\mathbf{x},t) \tag{35}$$

with domain $D = [0,\infty)^d$. Then for each component, the ergodic distribution is Gamma:

$$m_i(x_i) = \frac{\theta_i^{\beta_i+1}}{\Gamma(_i+1)} x_i^i e^{-\theta_i x_i},\ x_i > 0,$$

with

$$\beta_i = \frac{2a_i}{\sigma_{ii}^2} - 1,\ \ \theta_i = \frac{2b_i}{\sigma_{ii}^2}.$$

The boundary conditions are: $D_i^2 = +\infty$ is a natural boundary for all choices of parameters and

$$D_i^1 = \begin{cases} \text{exit}, & \beta_i \le -1 \\ \text{regular}, & -1 < \beta_i < 0 \\ \text{entrance} & 0 \le \beta i, \end{cases} \tag{36}$$

where $i = 1,\ldots,d$.

The corresponding eigenfunctions are Laguerre polynomials, $L_n^{(\alpha)}(x)$ [9] and $\lambda_n = n_1 + \cdots + n_2$.

The eigenvalue expansion for the transition probability density is given by

$$p(\mathbf{x};\mathbf{x}_0,t)=\prod_{i=1}^{d}m_i(x_i)\sum_{n_1=0}^{\infty}\cdots\sum_{n_d=0}^{\infty}\frac{e^{-(n_1b_1+\cdots+n_db_d)t}n_1!\times\cdots\times n_d!}{(\beta_1+1)_{n_1}\times\cdots\times(\beta_d+1)_{n_d}}\prod_{i=1}^{d}L_{n_i}^{(\beta_i)}(\theta_i x_{i,0})\prod_{i=1}^{d}L_{n_i}^{(\beta_i)}(\theta_i x_i)\,, \tag{37}$$

In this case also we can compare the analytical and numerical expectations of the time-dependent solutions using formula (34).

In Fig. 3 (a) we plot the numerical solution of the 2-D FPE (35) when it converges to the steady-state solution, obtained using a spectral approximation with $N = 80$. The model parameters were chosen to be $a_1 = 0.2$, $a_2 = 0.3$, $b_1 = 2$, $b_2 = 0.7$ and $\sigma_{11}^2 = 0.2$, $\sigma_{22}^2 = 0.4$, $x_0 = 2$. The boundary conditions are entrance. Two basis functions are sufficient to represent the solution at steady state with $\alpha_0 = 30.15153$, $\alpha_1 = 1.111 \times 10^{-3}$. The exact solution to the problem is shown in Fig. 3 (b) with the same parameters. Fig. 3 (c) presents a comparison between the numerical and analytical first moments (see (34)).

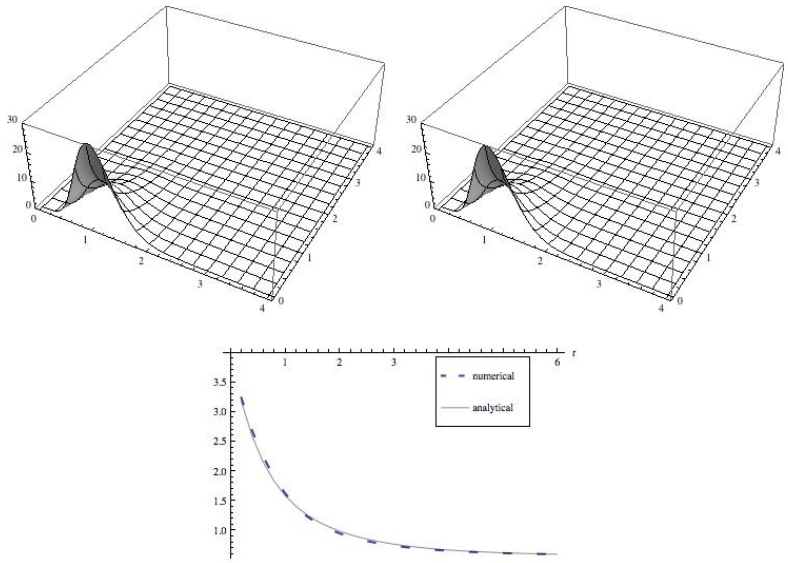

Figure 3. CIR process with $a_1 = 0.2$, $a_2 = 0.3$, $b_1 = 2$, $b_2 = 0.7$ and $\sigma_{11}^2 = 0.2$, $\sigma_{22}^2 = 0.4$, $x_0 = 2.6$. Boundary conditions are entrance . (a) Numerical approximation obtained using reduced basis approach. (b) Analytical solution. (c) Comparison between numerical and analytical expectations.

In Fig. 4 we plot the comparison between the expectations of the numerical solution in the case of the 4-D FPE (35) obtained using a spectral approximation with $N = 80$ and the analytical expression (34). The model parameters were chosen to be $a_1 = 2$, $a_2 = 3$, $a_3 = 4$, $a_4 = 4.5$, $b_1 = 2$, $b_2 = 4$, $b_3 = 5$, $b_4 = 2$ and $\sigma_{11}^2 = 0.2$, $\sigma_{22}^2 = 0.4$, $\sigma_{33}^2 = 0.7$, $\sigma_{44}^2 = 1$, $x_0 = 1.95$. At steady state only two basis functions are sufficient to represent the solution with $\alpha_0 = 96.7243$, $\alpha_1 = 4.7043 \times 10^{-7}$.

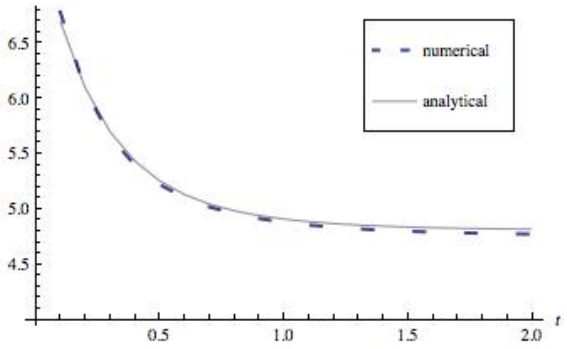

Figure 4. Comparison between the numerical and analytical expectations for CIR process in 4-D with $a_1 = 2$, $a_2 = 3$, $a_3 = 4$, $a_4 = 4.5$, $b_1 = 2$, $b_2 = 4$, $b_3 = 5$, $b_4 = 2$ and $\sigma_{11}^2 = 0.2$, $\sigma_{22}^2 = 0.4$, $\sigma_{33}^2 = 0.7$, $\sigma_{44}^2 = 1$, $x_0 = 1.95$.

4.3 The Jacobi diffusion

In financial mathematics, the Jacobi diffusion is used for modelling exchange rates in target zones [8].

In this case, the FPE is

$$\frac{\partial p(\mathbf{x},t)}{\partial t} = -\sum_{i=1}^{d} \frac{\partial}{\partial x_i}(a_i - b_i x_i)p(\mathbf{x},t) + \frac{1}{2}\sum_{i=1}^{d} \frac{\partial^2}{\partial x_i^2}\sigma_{ii}^2 x_i(A_i - x_i)p(\mathbf{x},t) \quad (38)$$

with domain $D = [0, A_i]^d$, $i = 1, \ldots, d$. The invariant density function for each component has the form

$$m_i\left(x_i\right) = \frac{x_i^{\beta_i}\left(A_i - x_i\right)^{\gamma_i}}{A_i^{\gamma_i+\beta_i+1} B^{(\gamma_i+1,\beta_i+1)}},\ x_i \in [0, A_i]\,,$$

where $B^{(\alpha_i,\beta_i)}$ is the beta distribution

$$B^{(\gamma,i\beta_i)} = \frac{\Gamma(\gamma_i)\Gamma(\beta_i)}{\Gamma(\gamma_i + \beta_i)}, \quad (39)$$

and

$$\gamma_i = \frac{2b_i}{\sigma_{ii}^2} - \frac{2a_i}{\sigma_{ii}^2 A_i} - 1,\ \beta_i = \frac{2a_i}{\sigma_{ii}^2 A_i} - 1,\ \gamma_i > -1,\ \beta_i > -1,\ i = 1, \ldots, d.$$

The boundary behaviour for the Jacobi process is the same as for CIR process

at the left boundary

$$D_i^1 = \begin{cases} \text{exit}, & \beta_i \leq -1 \\ \text{regular}, & -1 < \beta_i < 0 \\ \text{entrance}, & 0 \leq \beta_i. \end{cases} \tag{40}$$

The corresponding eigenfunctions are Jacobi polynomials and the discrete spectrum of the generator is

$$\lambda_n = \lambda_{n1}^{(1)} + \cdots + \lambda_{nd}^{(d)};\ \lambda_{ni}^{(i)} = \frac{\sigma_{ii}^2}{2} n_i \left(n_i - 1 + \frac{2b_i}{\sigma_{ii}^2} \right).$$

The eigenvalue expansion of the transition probability density can written as

$$p(\bar{x_1}; \bar{x}_0, t) = \prod_{i=1}^{d} m_i(x_i) \sum_{n_1=0}^{\infty} \cdots \sum_{n_d=0}^{\infty} \frac{e^{-(\lambda_{n1}^{(1)} + \cdots + \lambda_{nd}^{(d)})t}}{p_{n_i}^2} \prod_{i=1}^{d} P_n^{(\gamma_i, \beta_i)}(y_{i,0}) \prod_{i=1}^{d} P_n^{(\gamma_i, \beta_i)}(y_{i,1}), \tag{41}$$

where

$$p_{n_i}^2 = \frac{(\gamma_i + 1)_{n_i} (\beta_i + 1)_{n_i}}{(\gamma_i + \beta_i + 2)_{n_i - 1} (2n_i + \gamma_i + \beta_i + 1) n_i!},\ i = 1, \ldots, d,$$

$$y_{i,j} = \left(\frac{2x_{i,j}}{A_i} - 1 \right),\ j = 0, 1 \ and\ (m)_n = \frac{\Gamma(m+1)}{\Gamma(m-n+1)}.$$

Numerical results can be obtained in the same way as for the O-U and CIR processes.

4.4 Fisher-Snedecor diffusion

The corresponding FPE is

$$\frac{\partial p(\mathbf{x}, t)}{\partial t} = -\sum_{i=1}^{d} \frac{\partial}{\partial x_i} \left[-\theta_i (x_i - \frac{\beta_i}{\beta_i - 2}) \right] p(\mathbf{x}, t) + \frac{1}{2} \sum_{i=1}^{d} \frac{\partial^2}{\partial x_i^2} \left[\frac{4\theta_i}{\gamma_i (\beta_i - 2)} x_i (\gamma_i x_i + \beta_i) \right] p(\mathbf{x}, t). \tag{42}$$

where $\gamma_i > 0$, and $\beta_i > 2$ and $i = 1, \ldots, d$.

The invariant distribution for each component is Fisher-Snedecor $FS(\gamma_i, \beta_i)$:

$$m_i(x_i) = \frac{\gamma_i^{\gamma_i/2} \beta_i^{\beta_i/2}}{B(\frac{\gamma_i}{2}, \frac{\beta_i}{2})} \frac{x_i^{\frac{\gamma_i}{2} - 1}}{(\gamma_i x_i + \beta_i)^{\frac{\gamma_i}{2} + \frac{\beta_i}{2}}},\ x_i > 0,\ i = 1, \ldots, d, \tag{43}$$

and $B(\gamma_i, \beta_i)$ is the beta function, while γ_i and β_i are some shape parameters.

The restriction $\beta_i > 2$ on the value of the parameter β_i ensures the existence of the mean of the invariant distribution. Therefore, the quadratic polynomial $d(x_i) = x_i(\gamma_i x_i + \beta_i)$ with the positive first coefficient ($b_{i,2} > 0$) and positive discriminant $\Delta(d_i) > 0$ characterizes Fisher-Snedecor diffusion in the class of Pearson diffusions.

In this case, the negative infinitesimal generator ($-G$) has a finite set of simple eigenvalues:

$$\lambda_n = \lambda_{n1}^{(1)} + \cdots + \lambda_{nd}^{(d)};\ \lambda_{n_i}^{(i)} = \frac{\theta_i}{\beta_i - 2} n_i(\beta_i - 2n_i),\ 0 \le n_i \le \left[\frac{\beta_i}{4}\right],\ \beta_i > 2. \quad (44)$$

in $[0, \Lambda_i]^d$, and continuous part of the spectrum with cut off

$$\Lambda_i = \frac{\theta_i \beta_i^2}{8(\beta_i - 2)}. \quad (45)$$

The solution then can be written as

$$p(\mathbf{x};\ \mathbf{x}_0, t) = \prod_{i=1}^{d} m_i(x_i) \left[\sum_{n_1=0}^{\left[\frac{\beta_1}{4}\right]} \cdots \sum_{n_d=0}^{\left[\frac{\beta_d}{4}\right]} e^{-(\lambda_{n1}^{(1)} + \cdots + \lambda_{nd}^{(d)})t} \prod_{i=1}^{d} Q_{n_i}(x_{i,0}) \prod_{i=1}^{d} Q_{n_i}(x_i) \right.$$

$$\left. + \int_{\Lambda_1}^{\infty} \cdots \int_{\Lambda_d}^{\infty} e^{-(\lambda^{(1)} + \cdots + \lambda^{(d)})t} \prod_{i=1}^{d} \psi_i(x_{i,0}, -\lambda_i) \prod_{i=1}^{d} \psi_i(x_i, -\lambda_i) d\lambda_1 \ldots d\lambda_d \right], \quad (46)$$

where $Q_{n_i},\ i = 1, ..., d$, is a finite system of orthogonal polynomials [26] with respect to (43) and ψ_i are some special functions related to the hypergeometric functions ${}_2F_1$ and have a complicated form (see Meerschaert [27]). Thus, numerical methods seem inescapable.

We present some results in high-dimensions using the expectation. In Fig. 5 (a) we plot the numerical solution of the 2-D FPE (42) when it converges to the steady-state solution, obtained using a spectral approximation with $N = 80$. The model parameters were chosen to be $\gamma_1 = 1.8$, $\gamma_2 = 5$, $\beta_1 = 10$, $\beta_2 = 7$ and $\theta_1^2 = 0.5$, $\theta_2^2 = 0.2$. For the first dimension the boundary is natural and for the second dimension it is regular. Two basis functions represent the solution at the steady-state, $\alpha_0 = 3.818013$, $\alpha_1 = 4.05 \times 10^{-3}$. The exact solution to the problem is shown in Fig. 5 (b) with the same parameters.

Fig. 6 shows the transient expectation calculated for the numerical solution of the 4-D FPE (42). The following parameters are used here: $\gamma_1 = 1.8$, $\gamma_2 = 5$, $\gamma_3 = 3$, $\gamma_4 = 4$, $\beta_1 = 10$, $\beta_2 = 7$, $\beta_3 = 15$, $\beta_4 = 20$ and $\theta_1^2 = 0.5$, $\theta_2^2 = 0.2$,

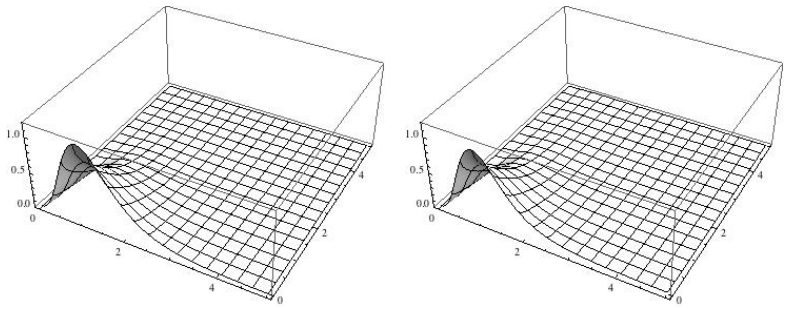

Figure 5. Fisher-Snedecor process at steady-state in 2-D with $\alpha_1 = 1.8$, $\alpha_2 = 5$, $\beta_1 = 10$, $\beta_2 = 7$ and $\theta_1^2 = 0.5$, $\theta_2^2 = 0.2$. (a) Numerical approximation obtained using reduced basis approach. (b) Analytical solution.

$\theta_3^2 = 1$, $\theta_4^2 = 0.7$ and only two basis function are sufficient to represent the solution with $\alpha_0 = 8.88770$, $\alpha_1 = 9.5 \times 10^{-6}$.

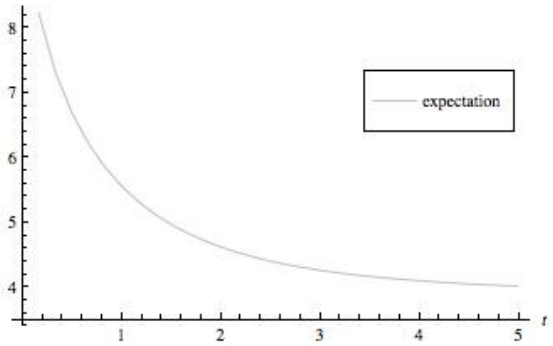

Figure 6. Transient expectations for the Fisher-Snedecor process in 4-D with $\gamma_1 = 1.8$, $\gamma_2 = 5$, $\gamma_3 = 3$, $\gamma_4 = 4$, $\beta_1 = 10$, $\beta_2 = 7$, $\beta_3 = 15$, $\beta_4 = 20$ and $\theta_1^2 = 0.5$, $\theta_2^2 = 0.2$, $\theta_3^2 = 1$, $\theta_4^2 = 0.7$

4.5 Reciprocal gamma diffusion

The corresponding FPE is

$$\frac{\partial p(\mathbf{x},t)}{\partial t} = -\sum_{i=1}^{d} \frac{\partial}{\partial x_i}\left[-\theta_i(x_i - \frac{\gamma_i}{\beta_i - 1})\right] p(\mathbf{x},t) + \frac{1}{2}\sum_{i=1}^{d} \frac{\partial^2}{\partial x_i^2}\left[\frac{2\theta_i}{(\beta_i-1)} x_i^{2,}\right] p(\mathbf{x},t), \tag{47}$$

where $\gamma_i > 0$ and $\beta_i > 1$ and $i = 1, \ldots, d$. The restriction $\beta_i > 1$ ensures the existence of the mean of the invariant distribution. In the one-dimensional case the equation in this form was first introduced by Shiryayev [36]. Peškir [34] and Øksendal [32] observed that SDEs of this type are one of the most popular short term interest rate models known as the Dothan model [10].

The invariant distribution of this diffusion for each component is reciprocal

gamma with the probability density function

$$m_i(x_i) = \frac{\gamma_i^{\beta_i}}{\Gamma(\beta_i)} x_i^{-\beta_i - 1} e^{-\frac{\gamma_i}{x_i}},\ x_i > 0,\ i = 1, \ldots, d \tag{48}$$

where $\gamma_i > 0$ and $\beta_i > 0$ are shape parameters. Moreover, the tail of the reciprocal gamma distribution with density (48) decreases like $x_i^{-(1+\beta_i)}$ and this distribution is heavy-tailed.

Therefore, the quadratic polynomial $d(x) = x^2$ with positive coefficient ($b_2 > 0$) and zero discriminant $\Delta(d) = 0$ characterizes the reciprocal gamma diffusion in the class of Pearson diffusion.

In this case, the negative infinitesimal generator ($-G$) has a finite set of simple eigenvalues

$$\lambda_n = \lambda_{n1}^{(1)} + \cdots + \lambda_{nd}^{(d)};\ \lambda_{n_i}^{(i)} = \theta_i n_i \left(\frac{\beta_i}{\beta_i - 1} - \frac{n_i}{\beta_i - 1} \right),\ 0 \le n_i \le \left[\frac{\beta_i}{2} \right],\ \beta_i > 1, \tag{49}$$

in $[0, \Lambda_i]^d$, where

$$\Lambda_i = \frac{\theta_i \beta_i^2}{4(\beta_i - 1)},\ i = 1, \ldots, d. \tag{50}$$

The solution can be represented in the form (46), where the corresponding polynomials that are orthogonal with respect to the density are the Bessel polynomials (see [25,26]). The boundary classification for this case has been described by Leonenko and Phillips [24]. For the derivation of the cutoff (50) see Meerschaert [27].

In Fig. 7 (a) we plot the numerical solution of the 2-D FPE (47) when it converges to the steady-state solution, obtained using a spectral approximation with $N = 80$. The model parameters were chosen to be $\gamma_1 = 2$, $\gamma_2 = 2$, $\beta_1 = 5$, $\beta_2 = 5$ and $\theta_1^2 = 1$, $\theta_2^2 = 1$. Two basis functions represent the steady-state solution, $\alpha_0 = 6.7450$, $\alpha_1 = 3.8 \times 10^{-4}$. The exact solution to the problem is shown in Fig.7 (b) with the same parameters.

Fig. 8 shows the transient expectation calculated for the numerical solution of the 3-D FPE (47). The following parameters are used here: $\gamma_1 = 2$, $\gamma_2 = 2$, $\gamma_3 = 3$, $\beta_1 = 3$, $\beta_2 = 5$, $\beta_3 = 6$, $\theta_1^2 = 1$, $\theta_2^2 = 1$, $\theta_3^2 = 1.2$, and two basis functions are sufficient to represent the steady-state solution with $\alpha_0 = 10.88397$, $\alpha_1 = 1.94 \times 10^{-3}$.

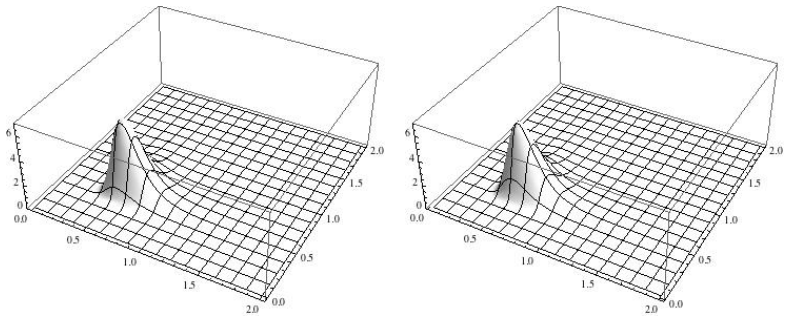

Figure 7. Reciprocal gamma process at steady-state in 2-D with $\gamma_1 = 2$, $\gamma_2 = 2$, $\beta_1 = 5$, $\beta_2 = 5$ and $\theta_1^2 = 1$, $\theta_2^2 = 1$. (a) Numerical approximation obtained using reduced basis approach. (b) Analytical solution.

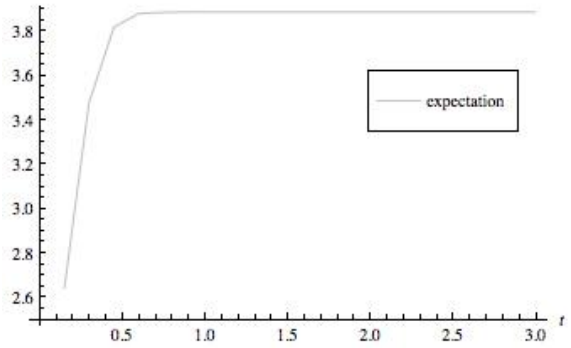

Figure 8. Transient expectations for reciprocal gamma process in 3-D with $\gamma_1 = 2$, $\gamma_2 = 2$, $\gamma_3 = 3$, $\beta_1 = 3$, $\beta_2 = 5$, $\beta_3 = 6$, and $\theta_1^2 = 1$, $\theta_2^2 = 1$, $\theta_3^2 = 1.2$.

4.6 Student diffusion

4.6.1 Symmetric version

The corresponding FPE is

$$\frac{\partial p(\mathbf{x},t)}{\partial t} = -\sum_{i=1}^{d} \frac{\partial}{\partial x_i}\left[-\theta_i(x_i-\mu_i)\right] p(\mathbf{x},t) + \frac{1}{2}\sum_{i=1}^{d} \frac{\partial^2}{\partial x_i^2}\left[\frac{2\theta_i\delta_i^2}{(\nu_i-1)}\left(1+\left(\frac{x_i-\mu_i}{\delta_i}\right)^2\right)\right] p(\mathbf{x},t), \tag{51}$$

where $\nu_i > 1$, $\delta_i > 0$, and $\mu_i \in R$ and $i = 1, \ldots, d$. Student diffusion was first studied by Wong, [38] in one dimension. This diffusion can also be observed as special case of the so-called hypergeometric diffusion introduced by Linetsky [25].

The invariant distribution of this diffusion is Student distribution for each component with the parameter $\nu_i > 1$ representing the degrees of freedom

with the probability density function

$$m_i(x_i) = \frac{\Gamma(\frac{\nu_i+1}{2})}{\delta_i\sqrt{\pi}\Gamma(\frac{\nu_i}{2})}\left(1+\left(\frac{x_i-\mu_i}{\delta_i}\right)^2\right)^{-\frac{\nu_i+1}{2}},\ x_i \in R,\ i=1,\ldots,d \qquad (52)$$

where $\delta_i > 0$ is a scale parameter and $\mu_i \in R$ is a location parameter.

Moreover, the left and right tails of the Student distribution with density (52) decrease like $|x_i|^{-(1+\nu_i)}$, and this distribution is heavy-tailed.

The quadratic polynomial in the one-dimensional case is $d(x) = 1+((x-\mu)/\delta)^2$ with positive first coefficient $b_2 > 0$ and negative discriminant ($\Delta(d) < 0$) characterizes the Student diffusion in the class of Pearson diffusions.

In this case, the negative infinitesimal generator ($-G$) has a finite set of simple eigenvalues

$$\lambda_n = \lambda_{n1}^{(1)} + \cdots + \lambda_{nd}^{(d)};\ \lambda_{n_i}^{(i)} = \frac{\theta_i}{\nu_i - 1} n_i(\nu_i - n_i),\ 0 \le n_i \le \left[\frac{\nu_i}{2}\right],\ \nu_i > 1 \quad (53)$$

in $[0, \Lambda_i]^d$, and where

$$\Lambda_i = \frac{\theta_i \nu_i^2}{4(\nu_i - 1)},\ \nu_i > 1,\ i = 1, \ldots, d. \qquad (54)$$

The solution can be represented in the form (52), where the corresponding polynomials orthogonal with respect to the density are Romanovski polynomials [25,27]. The boundary classification has been described in Leonenko and Phillips [24].

In Fig. 9 (a) we plot the numerical solution of the 2-D FPE (51) when it converges to the steady-state solution, obtained using a spectral approximation with $N = 80$. The model parameters were chosen to be $\mu_1 = 5$, $\mu_2 = 2$, $\delta_1 = 1$, $\delta_2 = 2$ and $\theta_1^2 = 1$, $\theta_2^2 = 1.5$, $\nu_1 = 9$, $\nu_2 = 15$. Two basis functions are sufficient to represent the steady-state solution with $\alpha_0 = 9.57888$, $\alpha_1 = 2.55\times10^{-6}$. The exact solution to the problem is shown in Fig. 9 (b) with the same parameters. Transient expectation is shown in Fig. 9 (c) with the same parameters.

In Fig. 10 we plot the expectation of the numerical solution of the 3-D FPE (51) with $N = 80$. The model parameters were chosen to be $\mu_1 = 5$, $\mu_2 = 2$, $\mu_3 = 4$,$\delta_1 = 1$, $\delta_2 = 2$, $\delta_3 = 1$ and $\theta_1^2 = 1$, $\theta_2^2 = 1.5$, $\theta_3^2 = 1$, $\nu_1 = 9$, $\nu_2 = 15$, $\nu_3 = 16$. Two basis functions represent the steady-state solution with $\alpha_0 = 2.7 - 5$, $\alpha_1 = 4.9765 - 14$.

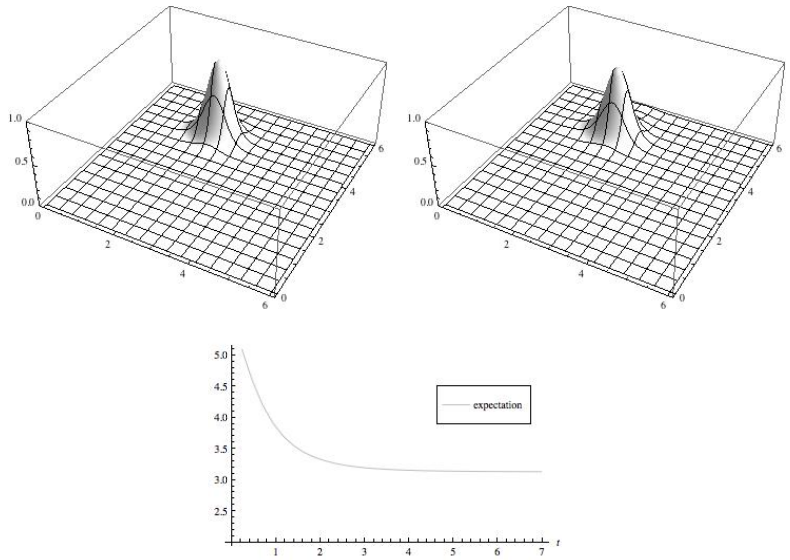

Figure 9. Student process at steady-state in 2-D with $\mu_1 = 5$, $\mu_2 = 2$, $\delta_1 = 1$, $\delta_2 = 2$ and $\theta_1^2 = 1$, $\theta_2^2 = 1.5$, $\nu_1 = 9$, $\nu_2 = 15$. (a) Numerical approximation obtained using reduced basis approach. (b) Analytical solution. (c) Transient expectation.

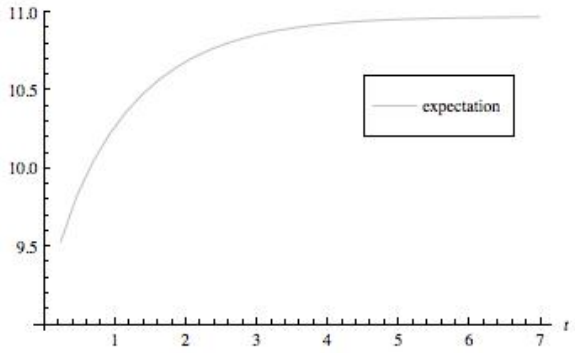

Figure 10. Transient expectation for Student process in 3-D with $\mu_1 = 5$, $\mu_2 = 2$, $\mu_3 = 4$,$\delta_1 = 1$, $\delta_2 = 2$, $\delta_3 = 1$ and $\theta_1^2 = 1$, $\theta_2^2 = 1.5$, $\theta_3^2 = 1$, $\nu_1 = 9$, $\nu_2 = 15$, $\nu_3 = 16$.

4.6.2 Skew-Student diffusion

Let us consider a more general version of the Student diffusion from our classification table. The corresponding FPE is

$$\frac{\partial p(\mathbf{x},t)}{\partial t} = -\sum_{i=1}^{d} \frac{\partial}{\partial x_i} \left[-\theta_i(x_i - \mu_i)\right] p(\mathbf{x},t) + \frac{1}{2} \sum_{i=1}^{d} \frac{\partial^2}{\partial x_i^2} \left[2\theta_i a_i \left(\delta_i^2 \left(x_i - \mu_i'\right)^2\right)\right] p(\mathbf{x},t). \tag{55}$$

where $\mu_i,\ \mu_i' \in R$ and $i = 1, \ldots, d$.

The ergodic distribution for each of the component has the form

$$m_i(x_i) = c(\mu_i, \mu_i', a_i, \delta_i) \frac{exp\left(\frac{\mu_i - \mu_i'}{a_i \delta_i} \cdot arctg\left(\frac{x_i - \mu_i'}{\delta_i}\right)\right)}{\left[1 + \left(\frac{x_i - \mu_i'}{\delta_i}\right)^2\right]^{\frac{1}{2a_i}+1}}, \tag{56}$$

for $x_i \in \mathbb{R},\ \mu_i, \mu_i' \in \mathbb{R},\ a_i > 0,\ \theta_i > 0,\ \delta_i > 0$, where

$$c(\mu_i, \mu_i', a_i, \delta_i) = \frac{\Gamma\left(1 + \frac{1}{2a_i}\right)}{\delta_i \sqrt{\pi} \Gamma\left(\frac{1}{2} + \frac{1}{2a_i}\right)} \prod_{k=0}^{\infty} \left[1 + \left(\frac{\frac{\mu_i - \mu_i'}{2a_i \delta_i}}{\nu_i + \frac{1}{2a_i} + k}\right)^2\right]^{-1}.$$

Note that in the symmetric case $\mu_i = \mu_i'$ and $\frac{\nu_i+1}{2} = \frac{1}{2a_i} + 1,\ i = 1, \ldots, d$. Thus, the ergodic distribution exists for $a_i > 0$. The boundaries are described similar to Student diffusion with the only difference is being that the Romanovski polynomials will depend on skewness.

The eigenvalues are represented below, see [25,27]:

$$\lambda_n = \lambda_{n1}^{(1)} + \cdots + \lambda_{nd}^{(d)};\ \lambda_{n_i}^{(i)} = \theta_i n_i \left[1 - a_i(n_i - 1)\right],\ 0 \le n_i \le \left[\frac{1 + a_i}{2a_i}\right].$$

In Fig. 11 (a) we plot the numerical solution of the 2-D FPE (55) when it converges to the steady-state solution, obtained using a spectral approximation with $N = 80$. The model parameters were chosen to be $\mu_1 = 4$, $\mu_2 = 8$, $\mu_1' = 9$, $\mu_2' = 14$, $\delta_1 = 0.5$, $\delta_2 = 1$ and $\theta_1 = 4$, $\theta_2 = 2$, $a_1 = 5$, $a_2 = 2$. Two basis functions represent the steady-state solution with $\alpha_0 = 1.7 \times 10^{-3}$, $\alpha_1 = 1.3737522 \times 10^{-16}$. The exact solution to the problem is shown in Fig.11 (b) with the same parameters. In Fig. 11 (c) the transient expectation is presented for the same parameters.

5 Discussion

In this paper six classes of high-dimensional Pearson diffusions have been considered. Numerical results have been presented that demonstrate the main features of the method when solving the FPE for each class. Previous investigations have been carried out on the multi-dimensional O-U, CIR, Jacobi processes, but none have been considered for the other three cases for heavy-tailed processes. One can see here the full potential of the reduced basis approach. This method is based on a separated representation of the distribution function and the use of an iterative scheme in which the basis is progressively enriched until the residual drops below a prescribed tolerance. Spectral discretisation

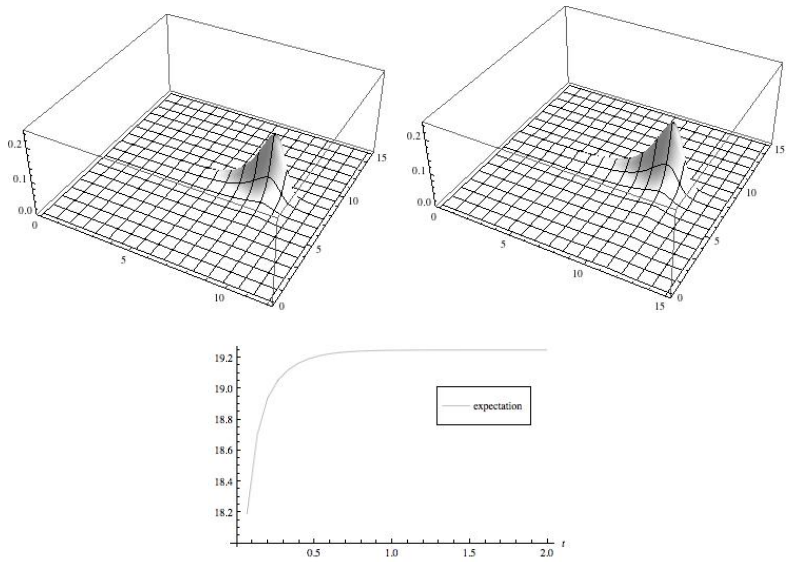

Figure 11. Non-symmetric Student process at the steady-state in 2-D with $\mu_1 = 4$, $\mu_2 = 8$, $\mu_1' = 9$, $\mu_2' = 14$, $\delta_1 = 0.5$, $\delta_2 = 1$ and $\theta_1 = 4$, $\theta_2 = 2$, $a_1 = 5$, $a_2 = 2$. (a) Numerical approximation obtained using the reduced basis approach. (b) Analytical solution. (c) Transient expectation.

of the basis functions is utilized and applied here for the multi-dimensional case. The number of degrees of freedom required for the solution was significantly reduced and as can be seen from the numerical examples presented in Section 5, two basis functions are sufficient to represent the solution. Please note, when using the scheme special attention should be paid to the domain in which FPE is solved (the distribution for each dimension should be one over the interval) and the boundary conditions.

In general, the solution of time-dependent multi-dimensional FPEs is a challenging problem. However, for a diagonal matrix in diffusion term (the Brownian motions of the multidimensional diffusions are independent) we can obtain reasonable results. In future we plan to consider multi-dimensional Pearson diffusions in the case when the full matrix in the diffusion term is present. This area of research is quite challenging and novel.

References

[1] Alcock, J. T., Burrage K., (2006), A note on the balanced method, BIT Numerical Mathematics, 46, 689-710.

[2] Alfonsi A., (2005), On the discretization schemes for the CIR (and Bessel squared) processes. Monte Carlo Methods and Applications, 11, N4, 355-384.

[3] Chen R.R., Scott, L., (2003), Multi-Factor Cox-Ingersoll-Ross Models of the Term Structure: Estimates and Tests from a Kalman Filter Model, Journal of

Real Estate Finance and Economics, 27, No2, 143-172.

[4] Ammar, A., Chinesta, F., Falco, A., Laso, M., (2007), On the reduction of stochastic kinetic theory models of complex fluids. Modelling Simul. Mater. Sci. Eng., 15, 639-652.

[5] Ammar, A., Mokdad, B., Chinesta, F., Keunings, R., (2006), A new family of solvers for some classes of multidimensional partial differential equations encountered in kinetic theory modeling of complex fluids, J. Non-Newtonian Fluid Mech., 139, 153-176.

[6] Andersen L., (2008), Simple and efficient simulation of the Heston stochastic volatility model, Journal of Computational Finance, 11, No3, 1-42.

[7] Bibby, B.M., Skovgaard, I.M. Sørensen, M. (2005). Diffusion-type models with given marginal distribution and autocorrelation function. Bernoulli 11: 281-299.

[8] Birge, J., Linetsky, V., Handbooks in operations research and management science: Financial Engineering, North-Holland, 2008.

[9] Chihara, T.S., (1978), An introduction to orthogonal polynomials, Gordon and Breach Science Publishers.

[10] Dothan, L.U., (1978), On the term structure of interest rate, J. Financ. Econ., 6, 59-69.

[11] Durn, A.J., Grnbaum, F.A., (2005), Structural formulas for orthogonal matrix polynomials satisfying second-order differential equations. I. Constr. Approx., 22, no.2, 255Đ271.

[12] Durn, A.J., Grnbaum, F.A., (2005), Orthogonal matrix polynomials, scalar-type Rodrigues' formulas and Pearson equations. J. Approx. Theory, 134, no.2, 267Đ280.

[13] Ethier, S., Kurtz, T., (1986), Markov processes, Characterization and Convergence, John Wiley, New York.

[14] Forman, J.L., Sørensen, M. (2008), The Pearson diffusions: A class of statistically tractable diffusion processes. Scand. J. Stat. 35: 438-465.

[15] Fulton, C. T., Pruess, S., Xie, Y., (2005), The automatic classification of Sturm-Liouvuille problems, Appl. Math. Comput., 124, 149-186.

[16] Gardiner, C.W., (2004), Handbook of stochastic methods for physics, Chemistry and the Natural Sciences, Third Edition, Springer, Berlin-New York, Tokyo.

[17] Gihman I.I., Skorohod, A.V., (1979), Stochastic differential equations, vol. III, Springer-Verlag, Berlin.

[18] Griffiths R.C., Spano, D., (2011), Multivariate Jacobi and Laguerre polynomials, infinite-dimansional extensions, and their probabilistic connections with multivariate Hahn and Meixner polynomials. Bernoulli 17(3), 1095-1125

[19] Itô, K., McKean, H., (1974), Diffusion processes and their sample paths, Springer, Heidelberg, Berlin.

[20] Kahl, C., (2002), Positive numerical integration of stochastic differential equations, Ph. D. thesis, Bergische University Wuppertal.

[21] Kahl, C., Schurz, H., (2006), Balanced Milstein methods for SDE's, Monte Carlo Methods and Applications, 12, N2, 143-170.

[22] Kumar, P., Narayanan, S., (2010), Modified path integration solution of Fokker-Planck equation: response and bifurcation of nonlinear systems, ASME J Comput Nonlinear Syn, 05, 1-12.

[23] Leonenko, G., Phillips, T.N., (2009), On the solution of the Fokker-Planck equation using high-order reduced basis approximation, Comp. Meth. Appl. Mech. Eng., 199, 158-168.

[24] Leonenko, G., Phillips, T.N., (2011), High-order approximation of Pearson diffusion processes, J. Comput. Appl. Math., accepted.

[25] Linetsky, V., (2004), The spectral decomposition of the option value, Int. J. Theor. Appl. Finance, 7, 337-384.

[26] Masjed-Jamei, M. (2004). Classical orthogonal polynomials with weight function $\left((ax+b)^2+(cx+d)^2\right)^{-p}\exp\left\{q\,\mathrm{arctg}\left((ax+b)/(cx+d)\right)\right\}$, $x\in\langle-\infty,\infty\rangle$ and generalisations of T and F distributions. *Integral Transforms and Special Functions* 15: 137-153.

[27] Meerschaert M.M., Sikorskii, A., (2012), Stochastic Models for Fractional Calculus, De Gruyter Studies in Mathematics, Studies in Mathematics 43, De Gruyter, Berlin.

[28] Milstein, G. N., Platen, E., Schirz, H., (1998), Balanced implicit method for stiff stochastic systems, SIAM J. Numer. Anal., 35, 1010-1019.

[29] Naess A., Moe, V., (2000), Efficient path integration method for non-linear dynamics systems, Probabilist. Eng. Mech., 15, 221-231.

[30] Novak, A., Stempak, K., (2006), L2-Theory of Riesz transforms for orthogonal expansions, J. Fourier Anal. Appl., 12 (6), 675-711.

[31] Novak, A., Sjogren P., (2008), Riesz transform for Jacobi expansions, Journal D'Analyse Mathematique, 104, 341-369.

[32] Øksendal, Bernt K., (2003), Stochastic differential equations, An Introduction with Applications, Berlin: Springer.

[33] Pearson, K., (1914), Tables for statisticians and biometricians, Cambridge University Press, Cambridge.

[34] Peškir, G., (2006), On the fundamental solution of the Kolmogorov-Shiryaev equation, From Stochastic Calculus to Mathematical Finance, Springer, 535 - 546.

[35] Platen, E., Rendek R., (2009), Exact scenario simulation for selected multi-dimensional stochastic processes. Communications on Stochastic Analysis, 3, N 3, 443-465.

bibitemkey-25-1Shaw, W., (2009), Dependency without Copulas or Ellipticity, European Journal of Finance, 15, 661 Ð 674.

[36] Shiryayev, A.N., (1961), The problem of the most rapid detection of a disturbance in a stationary process, Soviet. Math. Dokl., 2, 795-799.

[37] Shreve,S.E., (2004), Stochastic Calculus for Finance.II, Continuous-Time Models, Springer.

[38] Wong, E. (1964), The construction of a class of stationary Markoff Processes, In R. Bellman (Ed.), Sixteenth Symposium in Applied Mathematics - Stochastic Processes in Mathematical Physics and Engineering, pp. 264 – 276. Providence, RI: American Mathematical Society.